RESEARCH ARTICLE OPEN ACCESS

Chloroplast Vesiculation and Induced *Chloroplast Vesiculation* and *Senescence-Associated Gene 12* Expression During Tomato Flower Pedicel Abscission

Magda Tušek Žnidarič[1] | Maja Zagoršćak[1] | Živa Ramšak[1] | Katja Stare[1] | Marko Chersicola[1] | Maruša Pompe Novak[1,2] | Aleš Kladnik[3] | Marina Dermastia[1]

[1]Department of Biotechnology and Systems Biology, National Institute of Biology, Ljubljana, Slovenia | [2]School of Viticulture and Enology, University of Nova Gorica, Vipava, Slovenia | [3]Department of Biology, Biotechnical Faculty, University of Ljubljana, Ljubljana, Slovenia

Correspondence: Marina Dermastia (marina.dermastia@nib.si)

ABSTRACT

Abscission is a tightly regulated process in which plants shed unnecessary, infected, damaged, or aging organs, as well as ripe fruits, through predetermined abscission zones in response to developmental, hormonal, and environmental signals. Despite its importance, the underlying mechanisms remain incompletely understood. This study highlights the deleterious effects of abscission on chloroplast ultrastructure in the cells of the tomato flower pedicel abscission zone, revealing spatiotemporal differential gene expression and key transcriptional networks involved in chloroplast vesiculation during abscission. Significant changes in chloroplast structure and vesicle formation were observed 8 and 14 h after abscission induction, coinciding with the differential expression of vesiculation-related genes, particularly with upregulation of *Senescence-Associated Gene 12* (*SAG12*) and *Chloroplast Vesiculation* (*CV*). This suggests a possible vesicle transport of chloroplast degrading material for recycling by autophagy-independent senescence-associated vacuoles (SAVs) and CV-containing vesicles (CCVs). Ethylene signaling appears to be involved in the regulation of these processes, as treatment with a competitive inhibitor of ethylene action, 1-methylcyclopropene, delayed vesiculation, reduced the expression of *SAG12*, and increased expression of *Curvature Thylakoid 1A* (*CURT1A*). In addition, chloroplast vesiculation during abscission was associated with differential expression of photosynthesis-related genes, particularly those involved in light reactions, underscoring the possible functional impact of the observed structural changes. This work provides new insights into the molecular and ultrastructural mechanisms underlying abscission and offers potential new targets for agricultural or biotechnological applications.

1 | Introduction

The tomato fruit is an important source of essential vitamins, minerals, and fiber for human health and an important model organism for research on plants with fleshy fruits (Klee and Giovannoni 2011). It also serves as a model for developmental processes such as abscission (Bar-Dror et al. 2011; Ito and Nakano 2015). During abscission, plants shed unneeded,

---

infected, damaged, or senescent organs and ripe fruits in a systemically regulated manner. Abscission occurs in the pre-determined abscission zone (AZ) in response to developmental, hormonal, and environmental signals, but the complexity of the underlying anatomical, physiological, biochemical, and molecular mechanisms is not yet fully understood (Patterson et al. 2016).

The AZ of the tomato flower pedicel has been intensively studied over several decades due to its agricultural importance (Jensen, Valdovinos, and Jensen 1968; Bar-Dror et al. 2011; Dermastia et al. 2012; Liu et al. 2014; Sundaresan et al. 2016, 2020; Chersicola et al. 2017). As several findings emphasize that not all AZ cells behave the same (Bar-Dror et al. 2011; Dermastia et al. 2012; Chersicola et al. 2017), current research should focus on accurately linking molecular data to AZ physiology rather than applying non-AZ data to AZ. Using this new approach, two processes have been identified in tomato flower pedicel abscission: cell separation at the proximal side of the AZ and programmed cell death at its distal side. Both processes are associated with the action of ethylene and occur asymmetrically in the AZ (Bar-Dror et al. 2011; Dermastia et al. 2012; Chersicola et al. 2017).

Cell separation involves the dissolution of the middle lamella, the breakdown of the cell walls, and the subsequent formation of a protective layer (Roberts, Elliott, and Gonzalez-Carranza 2002). Key proteins and metabolites are released through vesicle trafficking to target the cell wall and middle lamella of differentiating cells within the AZ. Vesicle trafficking in the AZ of the tomato flower pedicel is accompanied by a remarkable increase in the expression of genes responsible for vesicle transport. These genes encode soluble N-ethylmaleimide-sensitive factor attachment protein receptors (SNAREs), SNARE regulators, and small GTPases (Sundaresan et al. 2020), which act by conventional protein secretion from the endoplasmic reticulum to the trans-Golgi network and plasma membrane (Wang et al. 2018). The proximal side of the AZ of the tomato leaf and flower pedicel is additionally characterized by endoreduplicated nuclei as well as the formation of cytoplasmic paramural bodies and various types of membrane vesicles containing electron-dense material (Bar-Dror et al. 2011; Dermastia et al. 2012; Chersicola et al. 2017) that could be related to unconventional protein secretion (Wang et al. 2018).

Abscission of plant organs is usually associated with their senescence (Roberts, Elliott, and Gonzalez-Carranza 2002), which is characterized by the transition from nutrient assimilation to remobilization of nutrients (Avila-Ospina et al. 2014). In senescent leaves, a crucial step of these catabolic processes is the degradation of chloroplasts and the recovery of their nitrogen content (Avila-Ospina et al. 2014). Autophagy is thought to play a central role in this chloroplast degradation process during senescence. During this process, cytoplasmic components are engulfed and transported by autophagosomes to the vacuole for recycling (Magen et al. 2022). In addition to autophagy, other mechanisms that are independent of the core autophagy machinery may also contribute to chloroplast breakdown. Senescence-associated vacuoles (SAVs) are specialized compartments that selectively degrade stromal chloroplast components and contain specific chloroplast components such as Rubisco and glutamine synthase but lack thylakoid proteins such as D1 and subunits of the reaction center of Photosystem II (Martínez et al. 2008; Gomez et al. 2019). Their main characteristics are cysteine protease activity and the presence of the senescence-associated protease *Senescence-Associated Gene 12* (SAG12) (Avila-Ospina et al. 2014). SAVs do not target the central vacuole but exhibit independent proteolytic activity (Martínez et al. 2008). In contrast to SAVs and autophagy, additional chloroplast vesiculation in Arabidopsis mobilizes chloroplast matrix, envelope, and thylakoid proteins into the vacuole for degradation. The marker protein for these vesicles is *Chloroplast Vesiculation* (CV), whose exact function is not known. Activation of the *CV* gene is induced by senescence and abiotic stress and leads to the formation of CV-containing vesicles (CCVs), which are then mobilized into the vacuole (Wang and Blumwald 2014). In addition, several peripheral vesicles in plastids, including chloroplasts, have been reported to play a role in ongoing, active, and protein-mediated vesicle transport in the context of thylakoid biogenesis (Lindquist and Aronsson 2018). The formation and accumulation of chloroplast vesicles associated with altered thylakoid membranes have been observed in mutants of chloroplast localized Rab GTPase CPRabA5e, Curvature Thylakoid 1 (CURT1) A and C, Thylakoid Formation 1 (THF1), and SNOWY COTYLEDON 2 (SCO2) proteins (Wang et al. 2004; Tanz et al. 2012; Armbruster et al. 2013; Karim et al. 2014). Small vacuoles and vesicles originating from unknown sources were also observed in the gradually degraded chloroplasts of tomato flower pedicel AZ (Chersicola et al. 2017).

There is a broad consensus on vesicle formation in response to stress in plant processes, based primarily on the identification of process-specific proteins in vesicle structures. However, the literature on the ultrastructure of these vesicles is remarkably sparse and the studies that do address vesiculation generally discuss its ultrastructure in the context of the initial reports. Moreover, vesiculation at the ultrastructural level during abscission has never been studied.

In this work, a detailed ultrastructural analysis of the chloroplasts and cytoplasmic vesicles in the proximal and distal sides of the flower pedicel of tomato AZ was performed, together with a detailed spatial and temporal transcriptional study of AZ genes to investigate a possible link between the chloroplast changes that follow the onset of flower pedicel abscission and the expression of genes putatively involved in vesiculation. In addition, the original transcriptomic data were reanalyzed (Sundaresan et al. 2016; Wilkinson et al. 2016) and combined with interaction network analysis to find new crosslinks between the signaling pathways involved in vesiculation during abscission processes. The results showed that two vesiculation processes that are independent of autophagy occurred during tomato flower pedicel abscission and are at least partially dependent on ethylene.

2 | Material and Methods

2.1 | Plant Material and Growing Conditions

The experimental conditions were as previously described (Chersicola et al. 2017). In brief, tomato plants (*Solanum lycopersicum* cv. VF36) were grown in growth chambers at 25°C,

75% humidity, and a 16/8-h day/night cycle. One day before sampling, all already opened flowers were removed from the plants so that only flowers that had opened the night before the experiments could be used. Flower clusters with up to four flowers were detached on the day of treatment and kept in 150-mL water in Erlenmeyer flasks.

2.2 | Treatment With 1-Methylcyclopropene (1-MCP)

The treatment of pedicels with 1-MCP was performed as previously described (Chersicola et al. 2017). The 1-MCP was prepared from 0.14% SmartFresh powder (AgroFresh Inc., Rohm and Haas Company, Philadelphia, United States) mixed with water (80 mg in 2 mL), resulting in an estimated concentration of 1000 ppb (v/v) of 1-MCP in the treatment chamber, according to the manufacturer's instructions. Half of the detached flower clusters were treated by exposing the flower clusters to an atmosphere of $1\,\mu L\,l^{-1}$ 1-MCP in 50-L airtight chambers for 2 h prior to the induction of abscission.

2.3 | Induction of Abscission and Sampling

Untreated pedicels of tomato flowers were sampled for gene expression and ultrastructural studies prior to abscission induction (0 h). Abscission was induced by removing flowers. In 1-MCP-treated flowers, abscission was also induced by removing flowers and further exposed to 1-MCP for 8 h. 1-MPC-treated and untreated abscission-induced pedicels were sampled after 8 h for gene expression and ultrastructure studies and after 14 h for ultrastructure observation only.

2.4 | Ultrastructural Analysis by Transmission Electron Microscope (TEM)

Details of sample preparation for TEM are described elsewhere (Bar-Dror et al. 2011; Chersicola et al. 2017). Pieces of plant tissue containing the AZ were fixed with glutaraldehyde and osmium tetroxide, embedded in Agar 100 resin, cut into ultrathin sections, and examined using the CM 100 TEM (Philips, Amsterdam, Netherlands). Images were captured with the ORIUS SC200 CCD camera (Gatan Inc., Washington DC, United States).

2.5 | Histological Sections and Laser Microdissection

The pedicels were excised with a razor blade and fixed in 3.7% formaldehyde, 50% ethanol, and 5% glacial acetic acid overnight at 4°C. Samples were then dehydrated through an increasing series of ethanol and tertiary butyl alcohol concentrations and embedded in Paraplast Plus (Sherwood Medical, United Kingdom). Then, 10-µm-thick longitudinal sections were cut with a rotary microtome (Autocut 2040 Reichert-Jung, Germany) and placed on MembraneSlide 1.0 PEN slides (Zeiss, Germany), deparaffinized in xylene, and the water removed from the tissue using 100% ethanol. Distal and proximal AZ regions as well as distal and proximal tissue regions outside the AZ of the pedicel were dissected from consecutive tissue slices ($n = 5$) using a laser microdissection microscope (PALM MicroBeam, Zeiss, Germany) and collected in AdhesiveCap 500 plastic tubes (Zeiss, Germany). The tubes were snap frozen in liquid nitrogen and stored at −80°C.

2.6 | Estimation of Vesicle and Thylakoid Volume Densities

Vesicles and thylakoids in chloroplasts were measured in TEM micrographs of chloroplasts. The number of chloroplast images examined was 23 for 0 h (control), 23 for 8 h, and 6 for 14 h after the flower pedicel abscission induction and 15 and 26 for 0 and 8 h after abscission induction in the presence of MCP. An unbiased point counting grid was overlayed over each chloroplast image in FIJI (Schindelin et al. 2012) using the Multipurpose grid.ijm macro (Mironov 2017). The chloroplast reference space was evaluated using sparse points corresponding to $0.16\,\mu m^2$ while the vesicles and thylakoids were evaluated using dense points corresponding to $0.01\,\mu m^2$. The relative structure volume (volume density) in the chloroplast reference space was calculated by dividing the area corresponding to points hitting the structure by the area of points in the entire chloroplast reference space. Data were imported and analyzed in R Version 4.3.3 (R Core Team 2023). Box plots were generated using the core R boxplot function, and difference between the group means was explored using the Kruskal–Wallis test followed by Dunnett's test with Šidák correction.

2.7 | Gene Expression

RT-qPCR was performed to assess the expression of five target genes associated with vesiculation: *SAG12*, *CV*, *CURT1A*, *CURT1B*, and *CURT1C*, using *Cytochrome C Oxidase* (*COX*) as previously validated reference gene (Bar-Dror et al. 2011; Müller et al. 2015) (Tables S1 and S2).

Total RNA was isolated from the collected tissue slices using RNeasy FFPE kits (Qiagen, Germany), according to the manufacturer's instructions. Quantitative reverse transcription real-time PCR (qPCR) was performed with samples from three biological replicates in a PCR machine (ViiA 7TM Real-Time PCR System, Applied Biosystems, Thermo Fisher Scientific, United States). Gene expression assays were designed using the Custom TaqMan Gene Expression Assays Service (Applied Biosystems, Thermo Fisher Scientific, United States). The expression assays and the reagents of the One-Step RT-PCR AgPath ID Mastermix (Life Technologies, Thermo Fisher Scientific, United States) were used according to the manufacturer's instructions. The qPCR was performed in a final reaction volume of $5\,\mu L$ containing $2\,\mu L$ RNA and $3\,\mu L$ reaction mix. The relative expression of the target and reference genes was determined using the standard curve quantification method. QuantGenius (http://quantgenious.nib.si) was used for quality control, standard curve–based relative gene expression quantification, and imputation of values below level of detection or quantification (LOD, LOQ) (Baebler et al. 2017).

2.8 | Data Analysis

Data analysis was performed in R (v4.3.2) (R Core Team 2023). A few missing values at random were imputed using random forest (R package missForest v1.5) (Stekhoven and Bühlmann 2012). The permutation-based *t*-test (R package MKinfer v1.1) (Kohl 2024) was used to denote differences between the specific treatment and the control within the corresponding tissue sections.

In addition, we reanalyzed transcriptomic data deposited in NCBI's Gene Expression Omnibus (Edgar, Domrachev, and Lash 2002) and accessible via GEO Accession Number GSE45355 (Sundaresan et al. 2016). Experiments using this microchip were performed exactly as the experiments in this study, and samples of the same cv. VF-36 were collected at the same time points after the induction of the flower pedicel abscission by flower removal. Analysis was performed for the comparisons of interest (time points 8 and 14h) using the interactive web tool GEO2R (with normalization and limma precision weighting options) (Barrett et al. 2013). The filtered results (adjusted *p* value < 0.05, (Table S3) were visualized in MapMan v3.7.0 (Usadel et al. 2009) using the ITAGv3.2 mapping file from GoMapMan (Ramšak et al. 2014).

Orthologue translation between Arabidopsis (query, proteome version Araport11) and tomato (subject, proteome version ITAG4.1) was performed using BLAST+ reciprocal best hit (RBH) search (R package orthologr v0.4.0) (Drost et al. 2015). For visualization purposes, orthologue pairs were prioritized based on scores, such as the highest identity, query, subject, and alignment length ratios, as well as ITAG3.2 and ITAG4.1 gene descriptions and MapMan annotations. In the case of many-to-many matches, when identical Arabidopsis identifiers matched identical tomato identifiers with similar scores, the identifiers were collapsed (Table S3).

In addition, using the Stress Knowledge Map (SKM) (Bleker et al. 2024), a subnetwork was created using the shortest path approach (R package igraph v1.5.1) (Csárdi and Nepusz 2006) between the nodes of interest (PCR estimated proteins, phytohormones and stress signaling molecules, and photosynthesis photosystem and phytochrome-related molecules), based on a ranking system for interaction reliability considering Ranks 0 (highest), 1, and 2 (Table S4) (Bleker et al. 2024). The experimental data were superimposed on a subnetwork and visualized in Cytoscape (v3.9.1) (Shannon et al. 2003).

3 | Results

3.1 | Significantly Altered Ultrastructure of Tomato Flower Pedicel Cells Is Associated With Vesicle Formation

The abscission of the tomato flower pedicel was generally accompanied by the appearance of different types of vesicles and small vacuoles (Figure 1B, C). Some of them, such as the paramural bodies (Figure 1D), have already been reported (Bar-Dror et al. 2011; Dermastia et al. 2012). In this study, we investigated the possible origin of other observed vesicles.

The increased formation of chloroplast vesicles up to 14h postabscission induction is accompanied by a reduction in thylakoid volume.
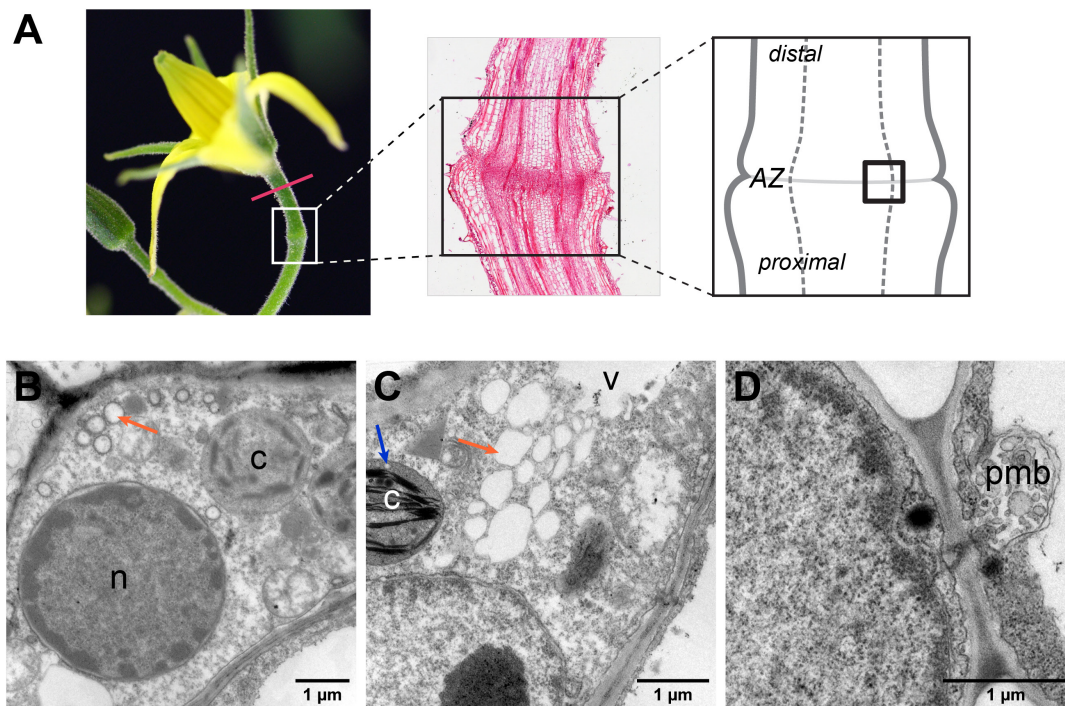

FIGURE 1 | Vesicles and vacuoles in the cells of the tomato flower pedicel abscission zone (AZ) following flower removal to induce abscission. (A) Schematic overview of the flower pedicel showing the abscission fracture plane from which the TEM micrographs were taken. Eight hours after abscission induction, various vesicles are visible in the cytoplasm (B, C) and within chloroplasts (C), as well as paramural bodies (D). Abbreviations: c, chloroplast; n, nucleus; v, vacuole; pmb, paramural body. Orange arrows indicate different types of vesicles in the cytoplasm, while the blue arrow marks vesicles located in the chloroplast.

Using TEM, we examined the extent of chloroplast changes in the tomato flower pedicel AZ, as well as on the distal and proximal sides of the AZ, 8 and 14h after abscission induction (Figure 2). Compared to the control at 0-h time point, some ultrastructural changes were visible in the thylakoids 8h after the abscission induction. These changes gradually increased over time, reaching a peak at approximately 14h after abscission induction, coinciding with the completion of AZ layer separation and termination of abscission (Meir et al. 2010; Chersicola et al. 2017). Notably, the vesicles were not present in the noninduced control (Figure 2A–C), and not all chloroplasts were affected simultaneously to the same extent. The phenotypic changes in chloroplasts on the distal and proximal sides of the AZ were largely similar. The most prominent alteration was the reorganization of thylakoid architecture, with grana stacks reorganizing faster than the stroma lamellae (Figure 2E–G, I, marked with yellow arrows). Progressive degradation of the thylakoids consistently coincided with the appearance of vesicles (Figure 2D–I). Eight hours after abscission induction, vesicles were observed aligning with the chloroplast envelope (Figure 2D–F). In the late phase of abscission, the most degraded chloroplasts exhibited vesicle distribution throughout the entire chloroplast stroma (Figure 2G–I). During vesiculation, the grana stacks became highly compressed, with minimal luminal space, while stromal lamellae were considerably shortened and densely compacted (Figure 2E–G, I, marked with yellow arrows).

Unbiased stereological analysis of TEM micrographs was used to estimate the volume density of vesicles and thylakoids within chloroplasts during abscission (Figure S1). After induction of abscission, vesicles were clearly visible and accounted for approximately $6\% \pm 1\%$ (mean $\pm$ SE) of the chloroplast volume at 8h, increasing to $12\% \pm 3\%$ by 14h (Figure S1A). Concurrently, thylakoid volume decreased significantly from $24\% \pm 1\%$ in control samples to $18\% \pm 2\%$ after the induction of abscission (Figure S1B).

Chloroplast vesicles were formed from several tubular structures located at the periphery of the thylakoid (Figure 3A). These vesicles eventually protruded from the edges of the thylakoid membrane and fused with the inner membrane of the chloroplast envelope (Figure 3A). In addition, budding vesicles were observed emerging from certain chloroplasts (Figure 3B).

3.2 | 1-MCP Treatment Delays Vesicle Formation

Since ethylene is necessary for abscission in both Arabidopsis and crop plants, we tested the hypothesis that some of the observed changes in the chloroplasts may be associated with action of ethylene. To investigate this, we pretreated detached flower clusters with 1-MCP, a competitive inhibitor of ethylene action, which is known to delay pedicel abscission for at least 20h (Meir et al. 2010). The effects of 1-MCP were assessed 8h after abscission induction. In comparison to samples where abscission was induced but not treated with 1-MCP, a trend
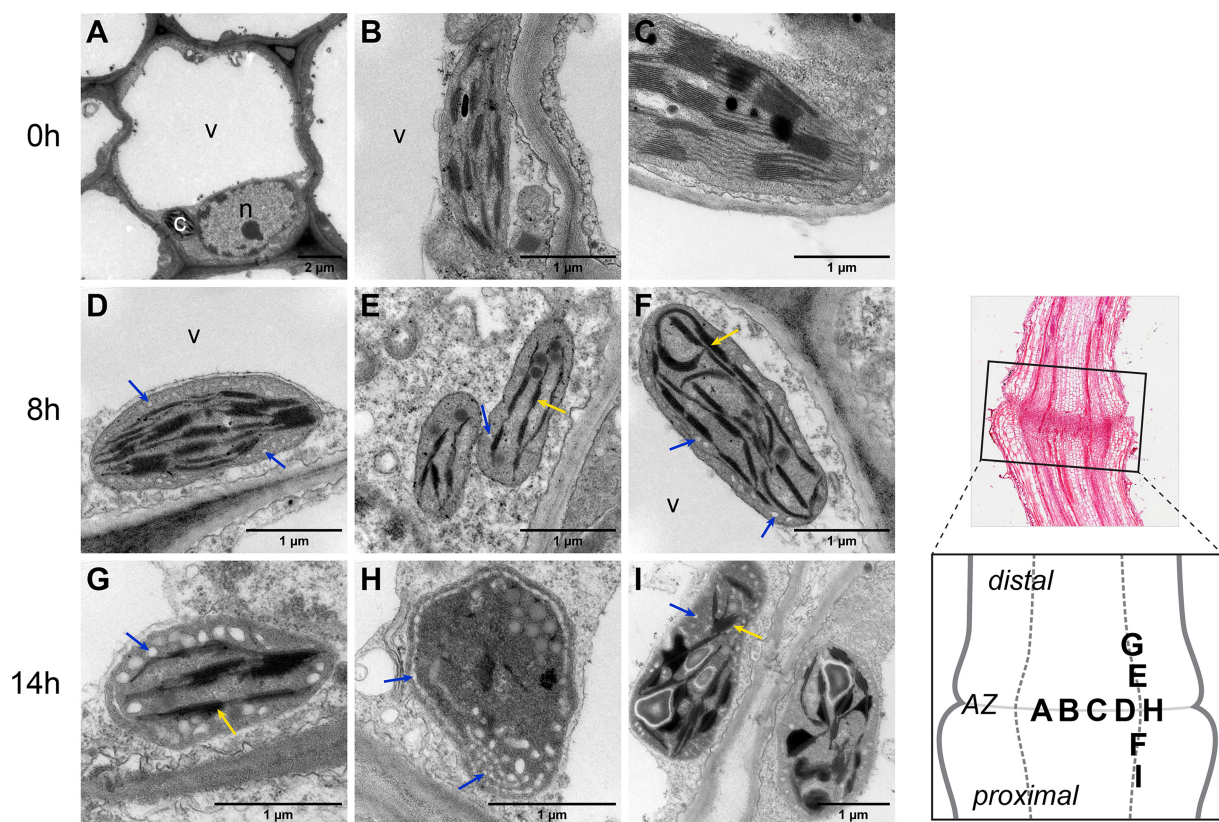

FIGURE 2 | Ultrastructure of chloroplast vesiculation during the induction of abscission in tomato flower pedicels. Tomato flower pedicels were sampled before abscission induction (0h, A–C) and at 8 (8h, D–F) and 14h after induction (14h, G–I). The locations of the TEM micrographs relative to the AZ are shown schematically (right). The letters A–I in the schematic overview correspond to the TEM micrographs, indicating the sampled parts of the pedicel. c, chloroplast; n, nucleus; v, vacuole. Blue arrows point to vesicles in chloroplasts, and yellow arrows point to altered thylakoids.
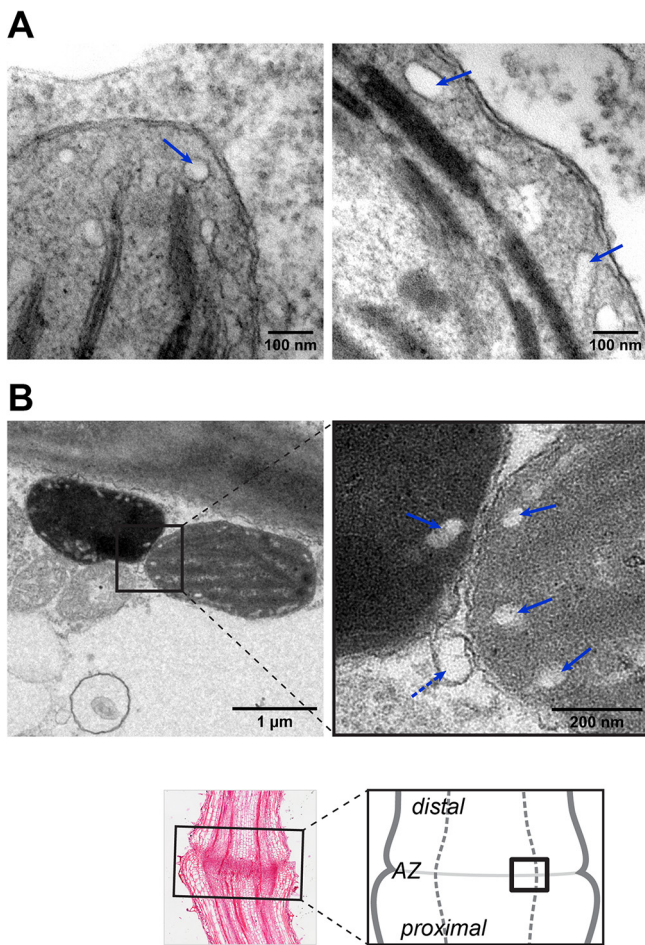
FIGURE 3 | Vesicle formation in chloroplasts of the tomato flower pedicel AZ. Vesicles pinch off from the thylakoids 14 h after abscission induction (A) and bud from the chloroplast (B). The abscission fracture plane, from which the TEM micrographs were taken, is shown schematically in the lower-left panel. v, vacuole. Solid blue arrows indicate vesicles within the chloroplasts, while the dotted blue arrow highlights a vesicle budding from the chloroplast.

of reduced vesicle formation in chloroplasts was observed (Figure 4).

3.3 | Differential Expression of Genes Associated With Vesiculation in AZ Is AZ Tissue Specific

Reanalysis of transcriptional metadata (Table S3) confirmed the differential expression of genes associated with chloroplast vesiculation in the AZ of tomato flower pedicels (Table 1), aligning with findings from other experimental systems not involved in the abscission process. Within 14 h following abscission induction, transcript levels of *SAG12* (Solyc02g076910) and *CV* (Solyc08g067630) showed substantial changes, with a 9-fold and 6.75-fold increase, respectively. However, this significant upregulation primarily occurred within the first 8 h, with only moderate increases between 8 and 14 h. This early transcriptional pattern was consistent across all genes examined. Eight hours after abscission induction, *CPRabA5e* and *SCO2/CYO1* were significantly upregulated, while *CURT1A*,
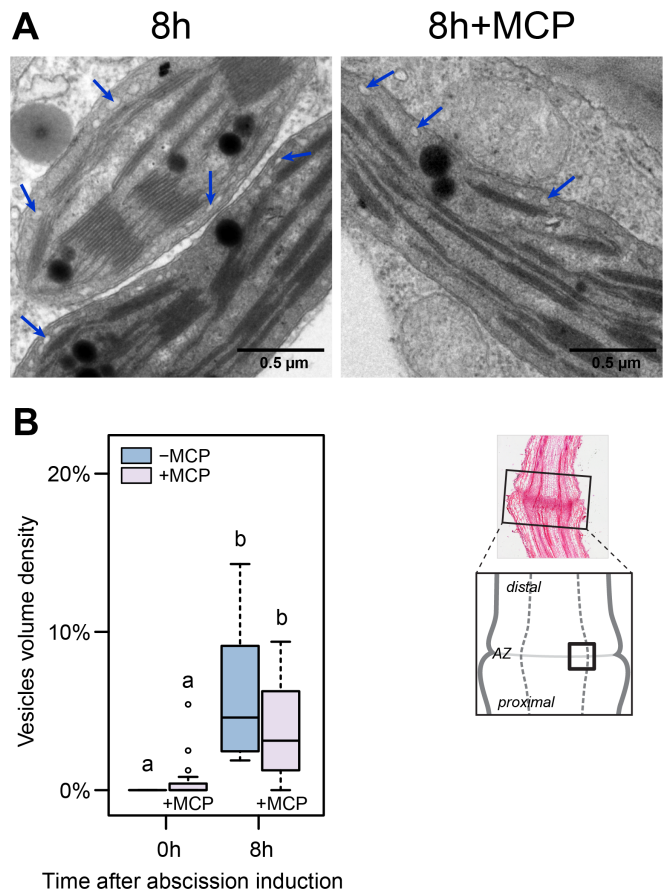

FIGURE 4 | Treatment with 1-MCP partially prevents vesiculation in the AZ. (A) Eight hours after abscission induction in samples treated with 1-MCP, the chloroplast structure remained unaffected, and fewer vesicles formed compared to the untreated control. The abscission fracture plane from which the TEM micrographs were taken is shown schematically (lower right). Blue arrows point to vesicles in chloroplasts. (B) Vesicle volume density in chloroplasts in the flower pedicel abscission zone following induction of abscission. The relative volume of vesicles was estimated using an unbiased point counting grid on TEM micrographs ($n = 23, 15, 23$, and 26 for 0 h − MCP, 0 h + MCP, 8 h − MCP, and 8 h + MCP, respectively) of individual chloroplasts. Differences between the group means were analyzed using the Kruskal–Wallis test followed by Dunnett's test with Šidák correction. Groups labeled with different letters have significantly different means ($p < 0.05$). Box plots show medians and interquartile ranges.

CURT1B, *CURT1D*, *CPSAR1*, and *Fuzzy onion-like* (*FZL*) were downregulated. No significant differential expression was observed for *CURT1C*, *THF1*, or *Vesicle-Inducing Protein in Plastids 1* (*VIPP1*) compared to the time point prior to abscission induction.

Building on our previous studies (Bar-Dror et al. 2011; Chersicola et al. 2017, 2018), which clearly showed the spatial separation of gene expression and corresponding proteins across cell layers in both the tomato leaf petiole and flower pedicel AZs, we further investigated the spatial transcriptional dynamics of five target genes related to chloroplast vesiculation using RT-qPCR. This analysis was conducted 8 h after abscission induction, a time point aligning with most of

TABLE 1 | List of genes putatively associated with vesiculation and differentially expressed in the tomato flower pedicel AZ at 8 and 14 h after abscission induction. Reanalysis of GSE45355 (Sundaresan et al. 2016) for comparisons of interest using Geo2R (Barrett et al. 2013). In the experiment, the AZ was not divided into individual layers. Fold changes (FC) calculated as $\log_2$FC are as follows: 8 versus 0, that is, 8 h after abscission induction compared to control before induction; 14 versus 0, that is, 14 h after abscission induction compared to control before induction; 14 versus 8, that is, 14 h after abscission induction compared to 8 h after induction. The color intensity corresponds to the extent of the fold changes. The relative expression levels are shown in red (upregulation) and blue (downregulation).

Gene ID	Gene name	8 vs. 0 $\log_2$FC	p	14 vs. 0 $\log_2$FC	p	14 vs. 8 $\log_2$FC	p
Solyc02g076910	*Sag12*	5.56	0.01240	9.18	0.00072	3.47	0.00467
Solyc08g067630	*CV*	5.66	0.00155	6.75	0.00041	1.11	0.02341
Solyc01g067530	*CPSAR1*	−1.34	0.00046	−1.48	0.00026	−0.12	0.75952
Solyc01g095430	*CURT1A*	−1.10	0.00134	−0.88	0.00837	0.21	0.46992
Solyc10g005050	*CURT1B*	−1.09	0.00049	−1.78	0.00001	−0.74	0.02552
Solyc06g066620	*CURT1C*	−0.23	0.45500	−0.48	0.13300	−0.28	0.16084
Solyc11g010480	*CURT1D*	−1.22	0.00073	−1.20	0.00051	0.01	0.98525
Solyc09g098170	*CPRabA5e*	0.67	0.00955	0.68	0.00205	0.01	0.97565
Solyc07g054820	*THF1*	0.19	0.46900	0.47	0.10800	0.30	0.24290
Solyc11g008990	*VIPP1*	0.13	0.51600	0.02	0.94800	−0.12	0.60415
Solyc09g065160	*FZL*	−1.59	0.00035	−1.64	0.00005	−0.03	0.93870
Solyc01g108200	*SCO2/CYO1*	1.34	0.00012	0.99	0.00064	−0.38	0.10695

the changes observed in the reanalyzed transcriptomic data. The experiment included both the proximal and distal AZs, as well as adjacent cell layers (Figure 5, Figure S2). While the overall gene expression trends mirrored those in the entire AZ (Table 1), several differences were in individual AZ tissues (Figure 5, Figure S2). Notably, these spatially distributed differences in gene expression were not accompanied by corresponding variations in vesicle formation within specific AZ cell layers at the ultrastructural level.

Eight hours after abscission induction, there was a significant downregulation of *CURT1A*. Within the AZ, *CURT1A* expression was notably lower than in the tissues proximal and distal to the AZ, with the lowest levels observed in the distal AZ (Figure 5A, Figure S2). In contrast, *CURT1B* and *CURT1C* showed only a moderate decrease within the AZ and proximal tissues, and their expression was slightly higher in distal tissues. *CV* and *SAG12* expression levels were elevated in all tissues compared to the uninduced control, with the highest levels found in the distal AZ (Figure 5A, Figure S2).

To explore the possible role of ethylene in regulating gene expression associated with vesiculation, we applied 1-MCP. In agreement with its known effect on delaying abscission (Meir et al. 2010), gene expression at the 8-h time point in 1-MCP-treated samples showed only slight differences from untreated controls at the 0-h time point (Figure 5B, Figure S2). However, 1-MCP treatment led to a slight increase in *CURT1A* expression in the proximal AZ. *CURT1B* was moderately upregulated in both proximal AZ and distal tissues, while *CURT1C* showed almost no differential expression. While 1-MCP had a limited effect on *CV* expression, it significantly reduced *SAG12* expression compared to untreated controls (Figure 5B, Figure S2).

When comparing untreated samples with those treated with 1-MCP at the 8-h time point, 1-MCP had a notable effect on *CURT1A* and *SAG12* expression. The treatment increased *CURT1A* expression while significantly decreasing that of *SAG12*, suggesting that these two genes are at least partially regulated by ethylene (Figure 5C, Figure S2).

3.4 | Functional Connections Between Genes Involved in Vesiculation

The interactivity of the different processes contributing to vesicle formation in the cells during the abscission process of the tomato flower pedicel was assessed using the SKM (Bleker et al. 2024) and visualized using Cytoscape (Shannon et al. 2003) (Figure 6, Table S4). SKM serves as a central hub for research on plant responses to stress and integrates knowledge from multiple sources, including recent research articles and established resources such as KEGG, STRING, MetaCyc, and AraCyc. Unlike other aggregated resources, SKM offers unique capabilities such as the conversion of biochemical knowledge into various mathematical models, the integration of multiomics experiments, and interactive access to constantly updated information.

We used SKM to consolidate existing knowledge on genes involved in flower pedicel abscission with data on chloroplast vesiculation collected during this study. This analysis provides partial insight into how the temporal transcriptional activity of specific genes affects interconnected genes and thereby influences the ultrastructure of chloroplast vesiculation. The analysis revealed three main subnetworks. SKM confirmed several known pathways associated with abscission, including IAAs, JAZs, EIN3, WRKY57, and MYC2, and paved the way to SAVs
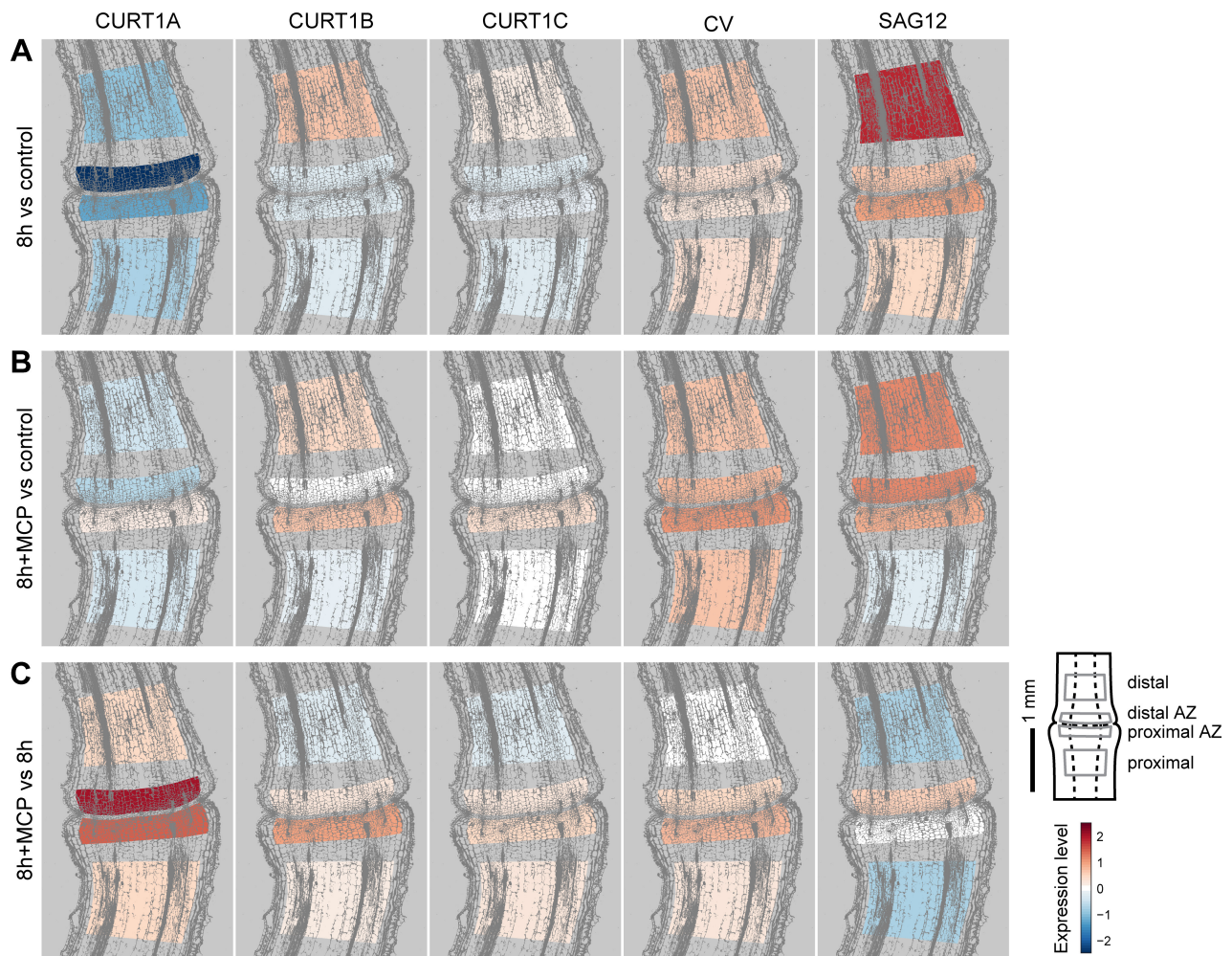
FIGURE 5 | Tissue-specific expression of genes associated with vesiculation 8 h after induction of tomato flower pedicel abscission in untreated samples and samples treated with 1-MCP. Expression of vesiculation-related genes was measured using qPCR in laser microdissected tissue samples from regions indicated in the schematic overview of the tomato flower pedicel. Relative expression levels are shown as fold change ($\log_2$FC). Red indicates upregulation, and blue indicates downregulation compared to control samples before abscission induction or untreated samples 8 h after abscission induction.

via the transcription factor WRKY57 and to CCVs via the transcription factor PIF4 (Figure 6). Like the expression patterns of vesiculation genes (Table 1), the main differential expression of genes in the revealed networks was observed at the 8-h time point (Figure 6).

3.5 | Light Reaction–Related Genes of Photosynthesis Are Affected During Tomato Flower Pedicel Abscission

To determine whether the observed changes in chloroplast structure during flower pedicel abscission correlate with differential expression of photosynthetic genes, the final list of differentially expressed genes (Table S3) was imported into the MapMan software (Usadel et al. 2009). This tool facilitates visually enhanced analysis by organizing the data into plant-specific biological processes and supporting ontology-based statistical analysis. This approach enables comprehensive biological interpretation and provides a global overview of the results. The analysis of

differentially expressed genes mapped to photosynthetic pathways revealed a significant impact, particularly on the light reactions of photosynthesis, at 8 and 14 h postabscission induction (Figure 7).

At the 8-h time point, several Photosystem II genes were upregulated, with the largest change (2.4-fold) observed in *CP47* (*Solyc01g050020*), which encodes a protein of the Photosystem II antenna complexes. In addition, transcripts of other members of the Photosystem II antenna complexes, *CP43* (*Solyc01g056470*, *Solyc10g018840*) and genes encoding Chlorophyll a/b-binding proteins (*Solyc03g005790*, *Solyc03g005770*), were also increased after abscission induction (Figure 7A, Table S3). However, other genes mapped to Photosystem II, including those encoding various Chlorophyll a/b-binding proteins, were downregulated. In contrast, genes mapped to Photosystem I, electron chain, and ATPases were mostly slightly downregulated 8 h after abscission induction. Between 8 and 14 h, almost all differentially expressed genes involved in light reactions were downregulated, especially those encoding Chlorophyll a/b-binding proteins (Figure 7B, Table S3).
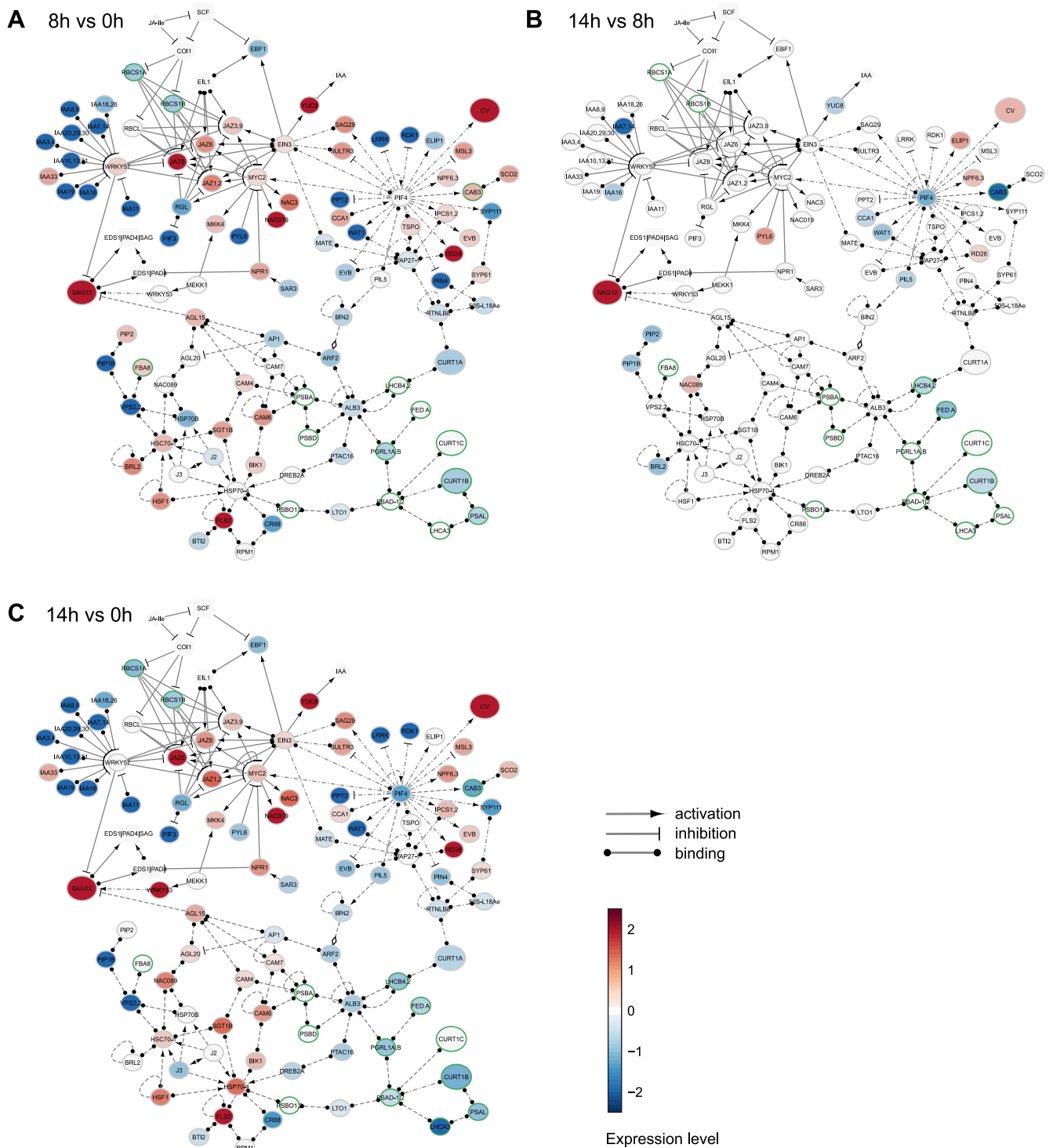
FIGURE 6 | Visualization of derived subnetworks involving chloroplast vesiculation, superimposed with tomato experimental data. Red represents upregulation, and blue represents downregulation in samples: (A) 8 h after abscission induction compared to control samples before abscission induction, (B) 14 h after abscission induction compared to 8 h after abscission induction, and (C) 14 h after abscission induction compared to control samples before abscission induction. Different line types (solid, dashed, and dash–dotted) represent different interaction type ranks (0, 1, and 2) (https://skm.nib.si/).

Notably, compared to the light reactions of photosynthesis, the genes involved in the Calvin cycle were less differentially regulated during flower pedicel abscission. Large-chain genes (*rbcL*) of ribulose-1,5-bisphosphate carboxylase (RuBisCO) (*Solyc11g013730*, *Solyc12g062540*, *Solyc07g021190*, *Solyc10g047430*, *Solyc02g077860*, *Solyc12g062560*,

Solyc07g021200, *Solyc04g039840*, *Solyc00g203660*, *Solyc01g007330*), which are encoded by chloroplast DNA and contain the active site responsible for nearly all carbon fixation on Earth (Kellogg and Juliano 1997), were only slightly, but not significantly, downregulated (Table S3). In contrast, genes encoding the small RuBisCO chains, imported from the cytosol
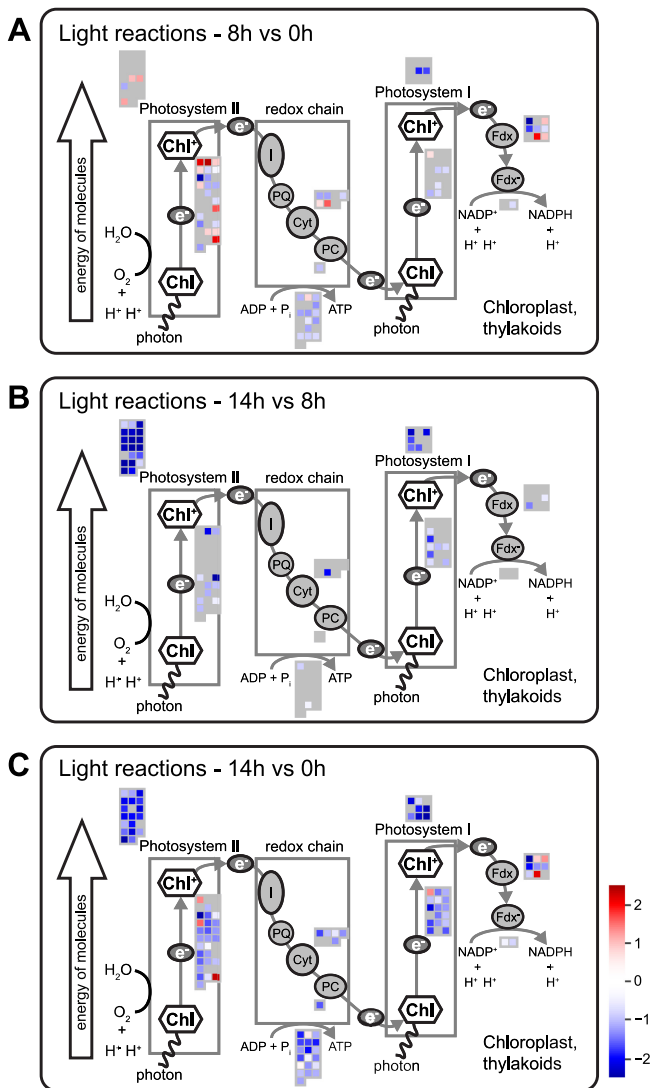
FIGURE 7 | Schematic representation of genes involved in the light reactions of photosynthesis 8 and 14 h after induction of tomato flower pedicel abscission. Each gene is represented by a colored square. Red indicates upregulation, and blue indicates downregulation compared to control samples before abscission induction: (A) 8 h after abscission induction, (B) 14 h after abscission induction compared to 8 h after induction, and (C) 14 h after abscission induction compared to control samples before induction. Only differentially expressed genes are shown. Data are from the list of genes differentially expressed in the tomato AZ flower pedicel at 8 and 14 h after abscission induction (Table S3). In this experiment, AZ was not divided into individual layers.

these transcriptional changes are part of the abscission process itself or a consequence of it.

4 | Discussion

4.1 | Old Observations, Rare Investigations

The vesiculation of chloroplast has already been observed since the earliest studies with TEM. For a long time, however, the prevailing opinion was that the vesicles were artifacts of sample preparation. Subsequent studies on wild-type plants and mutants, examined under different conditions such as ambient temperature (Morre et al. 1991) and presence or absence of inhibitory substances, have confirmed their consistent presence in chloroplasts (Lindquist and Aronsson 2018). These vesicles are thought to play a role in the assembly and maintenance of the inner chloroplast membranes. Structures similar to those described by this study were observed in early TEM micrographs from the late 1960s and early 1970s, appearing as invaginations of the inner chloroplast membrane or as cytoplasmic vesicles in the flower pedicel AZs of tomato and tobacco (Jensen and Valdovinos 1967; Valdovinos, Jensen, and Sicko 1972). While their potential role in the abscission process has never been directly investigated, abundant evidence from this and previous studies (Bar-Dror et al. 2011; Dermastia et al. 2012; Chersicola et al. 2017) suggests that vesicles in chloroplasts and the cytoplasm of tomato AZ cells are regularly associated with the abscission process. Nevertheless, it remains unclear whether these vesicles play an active role in abscission or are merely a byproduct of it.

Interestingly, despite the involvement of cell separation and programmed cell death in tomato abscission process, which are asymmetrically distributed within the AZ (Bar-Dror et al. 2011; Dermastia et al. 2012; Chersicola et al. 2017), no significant differences were detected in the number or morphology of vesicles formed at the proximal and distal AZ during abscission of the flower pedicel (Figure 2). However, a spatially differential distribution of gene expression associated with vesiculation was observed (Figure 5). This discrepancy could be attributed to the involvement of several other genes associated with vesicle formation during flower pedicel abscission, as identified through the SKM (Bleker et al. 2024) (Figure 6).

4.2 | Proteins Associated With Vesiculation During the Abscission Process

Several proteins are implicated in chloroplast vesicle transport, as mutant plants lacking or overexpressing these proteins show changes in the presence of vesicles (Wang et al. 2004; Tanz et al. 2012; Armbruster et al. 2013; Karim et al. 2014). However, their roles in abscission have never been explored. Our transcriptional reanalysis of genes involved in tomato flower pedicel abscission, associated with chloroplast vesiculation in prior studies, revealed differential expression of several key genes (Table 1).

The most significant finding was the strong induction of *CV* and *SAG12* genes, which are linked to autophagy-independent

into the stromal compartment of chloroplasts (*Solyc02g085950*, *Solyc03g034220*, *Solyc02g085940*), showed a significant decrease in transcript abundance (Table S3). Conversely, the *Solyc07g017950* gene, which also encodes a small RuBisCO chain, increased more than twofold (Table S3). The significance of these differences in gene expression remains unclear, given the limited understanding of the function of the small subunits (Badger and Sharwood 2023).

It is currently unknown whether or how these changes in photosynthesis-related gene expression are associated with the observed vesicle load. In addition, it remains unclear whether

degradation pathways involving CCVs and SAVs. *CV* encodes a chloroplast-targeted protein involved in both natural and stress-induced senescence (Wang and Blumwald 2014), accumulating in CCVs. These vesicles bud from chloroplasts and are then delivered to vacuoles for degradation, a process associated with swelling of thylakoid membranes and disassembly of the chloroplast. This mechanism involves interaction of CV with the Photosystem II subunit PsbO1 (Wang and Blumwald 2014) and with the clathrin heavy chain, facilitating vesicle transport from the inner chloroplast envelope membrane toward the cytosol (Pan et al. 2023). The latter step is suppressed by the oxidized glyceraldehyde-3-phospahte dehydrogenase (Pan et al. 2023). Supporting this, two genes encoding the clathrin heavy chain (*Solyc05g052510*, *Solyc06g051310*) and PsbO1 (*Solyc04g017770*) were upregulated during tomato flower pedicel abscission, while several genes encoding glyceraldehyde-3-phospahte dehydrogenase (*Solyc05g005820*, *Solyc06g071920*, *Solyc02g020940*, *Solyc12g094640*, *Solyc10g005510*, *Solyc04g009030*) were downregulated (Table S3). These findings suggest the observed vesicles during abscission induction might correspond to CCVs (Figures 2D–I and 3, marked with blue arrows). These vesicles, which budded from chloroplasts 8 h after abscission induction, appeared to aggregate in later stages of abscission, potentially as a response to abscission-related stress (Westphal, Soll, and Vothknecht 2001; Ahouvi et al. 2023). Gene encoding SAG12, the most common senescence-associated protease localized in SAVs (Martínez et al. 2008; Avila-Ospina et al. 2014), was strongly upregulated, suggesting that some vesicles observed in the cytoplasm of the AZ cells in the tomato flower pedicel might correspond to SAVs (Figure 1B, C, marked with orange arrows). Although the exact transfer mechanisms of chloroplast material into CCVs and SAVs remain poorly understood (Otegui et al. 2024), the upregulation of their marker genes indicates that both pathways play roles in degradation of chloroplast proteins during tomato flower pedicel abscission. This supports the existence of separate degradation pathways for Photosystem II and Photosystem I proteins during abscission. SAVs, for instance, are not involved in the degradation of Photosystem II proteins (Gomez et al. 2019), whereas CCVs interact with the Photosystem II subunit PsbO1, localized in the thylakoid membrane (Wang and Blumwald 2014). Several PsbO1-encoding genes were differentially expressed during abscission (*Solyc04g017770*, *Solyc07g032620*, *Solyc07g032610*, *Solyc00g005900*) (Table S3).

The expression of genes that encode CURT1 proteins, which are involved in thylakoid biogenesis by inducing membrane curvature and their mutants have altered thylakoid architecture (Armbruster et al. 2013), was also studied. Among *CURT1* genes, only *CURT1A* was significantly downregulated during the flower pedicel abscission (Table 1, Figure 5). While single *CURT1A* depletion is unlikely to explain high vesicle formation (since vesicular structures in chloroplasts appear only occasionally in double (*curt1ac*), triple (*curt1abc*), or quadruple (*curt1abcd*) mutants; Armbruster et al. 2013), the altered thylakoid structure observed after abscission induction—characterized by unstacked membrane regions and broader stacks with fewer layers (Figure 2E–G, I, marked with yellow arrows)—could be partially linked to *CURT1A* downregulation.

Other genes related to chloroplast vesiculation, including those involved in vesicle transport through the Golgi apparatus and post-Golgi trafficking pathways, were also differentially expressed in our study. For example, a gene *FZL* involved in vesicle trafficking (Liang et al. 2018), was downregulated during abscission (Table 1). A recent study on regulatory genes involved in vesicle trafficking during flower pedicel abscission shows the expression of SNARE receptors, SNARE regulators, and small GTPases (Sundaresan et al. 2020), including the orthologs of FZL. The role of these proteins in vesicle budding is supported by studies on CPSAR1 (Khan, Lindquist, and Aronsson 2013), a protein found in the chloroplast envelope, stroma, and vesicles (Garcia et al. 2010), and CPRabA5e, which participates in thylakoid biogenesis and vesicle transport and interacts with CURT1A and the light-harvesting Chlorophyll a/b-binding protein of Photosystem II (Lindquist and Aronsson 2018). The differential expression of *FZL*, *CPSAR1*, and *CPRabA5e*, as well as *CURT1* genes and genes encoding Chlorophyll a/b-binding proteins, suggests there is still an unexplored role during the abscission (Tables 1 and S3).

In addition, the gene expression of *SCO2* that encodes a protein disulfide isomerase localized in chloroplasts, thought to be involved in the integration of LHCB1 proteins in thylakoids, was also upregulated in AZ. The mutants *sco2* with disrupted chloroplast biogenesis also display increased vesicle formation (Tanz et al. 2012). Vesicles similar to those observed here have been reported in the Arabidopsis mutant lacking VIPP1 (Kroll et al. 2001) or THF1 (Huang et al. 2013), both of which influence thylakoid organization. However, insignificant changes in *VIPP1* and *THF1* expression, alongside undifferentiated *LHCB1* expression, make these proteins unlikely candidates for the observed vesicles (Figure 2).

Finally, we considered vesicular trafficking of chloroplast components into vacuole during the flower pedicel abscission via autophagy-dependent bodies involving the ATG8-interacting 1 protein (ATI1) (Michaeli et al. 2014). While three *ATG8* genes (*Solyc01g068060*, *Solyc02g080590*, *Solyc03g031650*) (Table S3), which play central role in autophagy (Bu et al. 2020), were significantly upregulated (Table S1), *ATI1* was not differentially expressed. In addition, one of the two genes encoding the other two proteins involved in the process of chlorophagy in the vacuole, *CHMP1B* (*Solyc03g121360*, *Solyc08g028770*) (Table S3), was down regulated, while *CHMP1A* was not differentially expressed. This suggests that vacuole chlorophagy is not an important mechanism during abscission.

4.3 | New Pathways Resulting From the Reconstructed Network Are the Basis for New Research

The reconstructed network of possible interactions between genes involved in vesiculation during abscission revealed interesting new pathways that can be analyzed in the future to elucidate the process of tomato flower pedicel abscission. The network shows three subnetworks loosely connected by the transcription factors WRKY57, PIF4, and AGL15 (Figure 6).

The first subnetwork which is connected to a convergence node for jasmonic acid and auxin-mediated signaling pathways is organized around WRKY57 (Jiang et al. 2014) and connects

*JAZ*s and *IAA* genes to *SAG12*. It shows that the senescence process as part of abscission is regulated by multiple developmental and environmental factors involving a crosstalk between jasmonic acid and auxin signaling, in which WRKY57 is a common component as a repressor of JA-induced leaf senescence. WRKY57 also represses the transcription of *SAG12* (Jiang et al. 2014). The strong induction of *SAG12* expression during tomato flower pedicel abscission was consistent with only slight upregulation of *WRKY57* 8 h after abscission induction and no differential expression 14 h after abscission induction (Figure 6).

This subnetwork is loosely connected to the second subnetwork through the transcription factors EIN3, a key regulator of ethylene signaling (Dolgikh, Pukhovaya, and Zemlyanskaya 2019), and MYC2 (Luo et al. 2023) (Figure 6), a key transcriptional regulator of JA-induced gene activation. In the second subnetwork, several genes, including *CV,* are clustered around the transcription factor PHYTOCHROME-INTERACTING FACTOR 4 (PIF4) from the bHLH (basic helix–loop–helix) family of transcription factors (Figure 6). PIFs play a crucial role in various signaling pathways, such as responses to abiotic and biotic stress, hormone signaling, temperature-induced responses, and developmental processes such as senescence and seed and fruit development (Xu and Zhu 2021; Sharma et al. 2023). Many recent reports show that PIF4 is directly associated with many of its target genes to modulate global transcriptome gene expression levels and is involved in many developmental processes such as senescence via phytochrome signaling (Xu and Zhu 2021; Sharma et al. 2023). PIF4 has been reported to promote heat-induced leaf senescence by enhancing the expression of genes such as *IAA29 and IAA19*, among others. These results are consistent with the time point 8 h after abscission induction, when PIF4 was not differentially expressed, but *IAA29* and *IAA19* were significantly downregulated, while *CV* was upregulated (Figure 6A). Fourteen hours after abscission induction, PIF4 was downregulated consistent with lower CV transcript and nondifferentially expressed IAA29 and IAA19 (Figure 6B).

The third subnetwork bridges the first subnetwork with *CURT1* genes and is connected to the second subnetwork via the MADS domain transcription factor *AGAMOUS-LIKE 15* (AGL15) (Figure 6). AGL15 is an important transcription factor that regulates abscission (Patharkar and Walker 2018) and is a negative regulator of abscission when it transiently accumulates in flower buds (Fernandez et al. 2000). It has been shown that the breaking strength of petals initially decreased but was then maintained at an intermediate value over a longer period of time. Abscission-related gene expression and structural changes were also altered in the presence of ectopic AGL15 (Fernandez et al. 2000). *AGL15* showed a similar temporal expression pattern to *WRKY57* during the abscission of the tomato flower pedicel (Figure 6).

5 | Conclusions

The discovery and confirmation of chloroplast vesiculation have greatly enhanced our understanding of chloroplast structure and function. Initially dismissed as artifacts, these vesicles have now been consistently observed in various plastids of both wild-type and mutant plants under diverse conditions, emphasizing their biological importance. This study revealed their potential role in abscission, a process that is crucial for plant development and response to environmental stimuli. While further studies are needed, it is notable that the expression of *SAG12* and *CURT1A* genes appears to be at least partially regulated by ethylene, and the inhibition of ethylene action by 1-MCP delayed chloroplast vesicle formation. Exploring the functional significance of chloroplast vesiculation, particularly in the context of abscission, could provide valuable insights into its role beyond membrane dynamics. Understanding its involvement in processes like abscission opens promising avenues to enhance our knowledge of plant biology and identify targets for agricultural or biotechnological applications.

References

Ahouvi, Y., Z. Haber, Y. Y. Zach, et al. 2023. "The Alteration of Tomato Chloroplast Vesiculation Positively Affects Whole-Plant Source–Sink Relations and Fruit Metabolism Under Stress Conditions." *Plant and Cell Physiology* 63: 2008–2026.

Armbruster, U., M. Labs, M. Pribil, et al. 2013. "Arabidopsis CURVATURE THYLAKOID1 Proteins Modify Thylakoid Architecture by Inducing Membrane Curvature." *Plant Cell* 25: 2661–2678.

Avila-Ospina, L., M. Moison, K. Yoshimoto, and C. Masclaux-Daubresse. 2014. "Autophagy, Plant Senescence, and Nutrient Recycling." *Journal of Experimental Botany* 65: 3799–3811.

Badger, M. R., and R. E. Sharwood. 2023. "Rubisco, the Imperfect Winner: It's All About the Base." *Journal of Experimental Botany* 74: 562–580.

Baebler, Š., M. Svalina, M. Petek, et al. 2017. "QuantGenius: Implementation of a Decision Support System for qPCR-Based Gene Quantification." *BMC Bioinformatics* 18: 276.

Bar-Dror, T., M. Dermastia, A. Kladnik, et al. 2011. "Programmed Cell Death Occurs Asymmetrically During Abscission in Tomato." *Plant Cell* 23: 4146–4163.

Barrett, T., S. E. Wilhite, P. Ledoux, et al. 2013. "NCBI GEO: Archive for Functional Genomics Data Sets--Update." *Nucleic Acids Research* 41: D991–D995.

Bleker, C., Ž. Ramšak, A. Bittner, et al. 2024. "A Knowledge Graph Resource for Systems Biology Analysis of Plant Stress Responses." *Plant Communications* 5: 100920.

Bu, F., M. Yang, X. Guo, W. Huang, and L. Chen. 2020. "Multiple Functions of ATG8 Family Proteins in Plant Autophagy." *Frontiers in Cell and Developmental Biology* 8: 466.

Chersicola, M., A. Kladnik, M. Tušek Žnidarič, A. Lers, and M. Dermastia. 2018. "The Pattern of 1-Aminocyclopropane-1-Carboxyl ate Oxidase Induction in the Tomato Leaf Petiole Abscission Zone Is Independent of Expression of the Ribonuclease-LX-Encoding *LeLX* Gene (B Hause, Ed.)." *Plant Biology* 20: 722–728.

Chersicola, M., A. Kladnik, M. T. Žnidarič, et al. 2017. "1-Aminocycl opropane-1-Carboxylate Oxidase Induction in Tomato Flower Pedicel Phloem and Abscission Related Processes Are Differentially Sensitive to Ethylene." *Frontiers in Plant Science* 8: 464.

Csárdi, G., and T. Nepusz. 2006. "The Igraph Software Package for Complex Network Research." *InterJournal, Complex Systems*: 1–9. https://api.semanticscholar.org/CorpusID:16923281.

Dermastia, M., A. Kladnik, T. Bar-Dror, and A. Lers. 2012. "Endoreduplication Preferentially Occurs at the Proximal Side of the Abscission Zone During Abscission of Tomato Leaf." *Plant Signaling & Behavior* 7: 1106–1109.

Dolgikh, V. A., E. M. Pukhovaya, and E. V. Zemlyanskaya. 2019. "Shaping Ethylene Response: The Role of EIN3/EIL1 Ttranscription Factors." *Frontiers in Plant Science* 10: 468867.

Drost, H. G., A. Gabel, I. Grosse, and M. Quint. 2015. "Evidence for Active Maintenance of Phylotranscriptomic Hourglass Patterns in Animal and Plant Embryogenesis." *Molecular Biology and Evolution* 32: 1221–1231.

Edgar, R., M. Domrachev, and A. E. Lash. 2002. "Gene Expression Omnibus: NCBI Gene Expression and Hybridization Array Data Repository." *Nucleic Acids Research* 30: 207–210.

Fernandez, D. E., G. R. Heck, S. E. Perry, S. E. Patterson, A. B. Bleecker, and S. C. Fang. 2000. "The Embryo MADS Domain Factor AGL15 Acts Postembryonically. Inhibition of Perianth Senescence and Abscission via Constitutive Expression." *Plant Cell* 12: 183–197.

Garcia, C., N. Z. Khan, U. Nannmark, and H. Aronsson. 2010. "The Chloroplast Protein CPSAR1, Dually Localized in the Stroma and the Inner Envelope Membrane, Is Involved in Thylakoid Biogenesis." *Plant Journal* 63: 73–85.

Gomez, F. M., C. A. Carrión, M. L. Costa, et al. 2019. "Extra-Plastidial Degradation of Chlorophyll and Photosystem I in Tobacco Leaves Involving 'Senescence-Associated Vacuoles'." *Plant Journal* 99: 465–477.

Huang, W., Q. Chen, Y. Zhu, et al. 2013. "Arabidopsis Thylakoid Formation 1 Is a Critical Regulator for Dynamics of PSII–LHCII Complexes in Leaf Senescence and Excess Light." *Molecular Plant* 6: 1673–1691.

Ito, Y., and T. Nakano. 2015. "Development and Regulation of Pedicel Abscission in Tomato." *Frontiers in Plant Science* 6: 442.

Jensen, T. E., and J. G. Valdovinos. 1967. "Fine Structure of Abscission Zones: I. Abscission Zones of the Pedicels of Tobacco and Tomato Flowers at Anthesis." *Planta* 77: 298–318.

Jensen, T. E., J. G. Valdovinos, and T. E. Jensen. 1968. "Fine Structure of Abscission Zones: II. Cell-Wall Changes in Abscising Pedicels of Tobacco and Tomato Flowers." *Planta* 83: 295–302.

Jiang, Y., G. Liang, S. Yang, and D. Yu. 2014. "Arabidopsis WRKY57 Functions as a Node of Convergence for Jasmonic Acid- and Auxin-Mediated Signaling in Jasmonic Acid-Induced Leaf Senescence." *Plant Cell* 26: 230–245.

Karim, S., M. Alezzawi, C. Garcia-Petit, et al. 2014. "A Novel Chloroplast Localized Rab GTPase Protein CPRabA5e Is Involved in Stress, Development, Thylakoid Biogenesis and Vesicle Transport in Arabidopsis." *Plant Molecular Biology* 84: 675–692.

Kellogg, E. A., and N. D. Juliano. 1997. "The Structure and Function of RuBisCO and Their Implications for Systematic Studies." *American Journal of Botany* 84: 413–428.

Khan, N. Z., E. Lindquist, and H. Aronsson. 2013. "New Putative Chloroplast Vesicle Transport Components and Cargo Proteins Revealed Using a Bioinformatics Approach: An Arabidopsis Model." *PLoS ONE* 8: e59898.

Klee, H. J., and J. J. Giovannoni. 2011. "Genetics and Control of Tomato Fruit Ripening and Quality Attributes." *Annual Review of Genetics* 45: 41–59.

Kohl M. 2024. Package 'MKinfer'.

Kroll, D., K. Meierhoff, N. Bechtold, et al. 2001. "VIPP1, a Nuclear Gene of Arabidopsis Thaliana Essential for Thylakoid Membrane Formation." *Proceedings of the National Academy of Sciences of the United States of America* 98: 4238–4242.

Liang, Z., N. Zhu, K. K. Mai, et al. 2018. "Thylakoid-Bound Polysomes and a Dynamin-Related Protein, FZL, Mediate Critical Stages of the Linear Chloroplast Biogenesis Program in Greening Arabidopsis Cotyledons." *Plant Cell* 30: 1476–1495.

Lindquist, E., and H. Aronsson. 2018. "Chloroplast Vesicle Transport." *Photosynthesis Research* 138: 361–371.

Liu, D., D. Wang, Z. Qin, et al. 2014. "The SEPALLATA MADS-Box Protein SLMBP21 Forms Protein Complexes With JOINTLESS and MACROCALYX as a Transcription Activator for Development of the Tomato Flower Abscission Zone." *Plant Journal* 77: 284–296.

Luo, L., Y. Wang, L. Qiu, et al. 2023. "MYC2: A Master Switch for Plant Physiological Processes and Specialized Metabolite Synthesis." *International Journal of Molecular Sciences* 24: 3511.

Magen, S., H. Seybold, D. Laloum, and T. Avin-Wittenberg. 2022. "Metabolism and Autophagy in Plants—A Perfect Match." *FEBS Letters* 596: 2133–2151.

Martínez, D. E., M. L. Costa, F. M. Gomez, M. S. Otegui, and J. J. Guiamet. 2008. "'Senescence-Associated Vacuoles' Are Involved in the Degradation of Chloroplast Proteins in Tobacco Leaves." *Plant Journal* 56: 196–206.

Meir, S., S. Philosoph-Hadas, S. Sundaresan, et al. 2010. "Microarray Analysis of the Abscission-Related Transcriptome in the Tomato Flower Abscission Zone in Response to Auxin Depletion." *Plant Physiology* 154: 1929–1956.

Michaeli, S., A. Honig, H. Levanony, H. Peled-Zehavi, and G. Galili. 2014. "Arabidopsis ATG8-INTERACTING PROTEIN1 Is Involved in Autophagy-Dependent Vesicular Trafficking of Plastid Proteins to the Vacuole." *Plant Cell* 26: 4084–4101.

Mironov, A. 2017. "Stereological Morphometric Grids for ImageJ." *Ultrastructural Pathology* 41: 126–126.

Morre, D. J., G. Seliden, C. Sundqvist, and A. S. Sandelius. 1991. "Stromal Low Temperature Compartment Derived From the Inner Membrane of the Chloroplast Envelope." *Plant Physiology* 97: 1558–1564.

Müller, O. A., J. Grau, S. Thieme, et al. 2015. "Genome-Wide Identification and Validation of Reference Genes in Infected Tomato Leaves for Quantitative RT-PCR Analyses (Y-W He, Ed.)." *PLoS ONE* 10: e0136499.

Otegui, M. S., C. Steelheart, W. Ma, et al. 2024. "Vacuolar Degradation of Plant Organelles." *Plant Cell* 36: 3036–3056.

Pan, T., Y. Liu, X. Hu, et al. 2023. "Stress-Induced Endocytosis From Chloroplast Inner Envelope Membrane Is Mediated by *CHLOROPLAST VESICULATION* but Inhibited by GAPC." *Cell Reports* 42: 113208.

Patharkar, O. R., and J. C. Walker. 2018. "Advances in Abscission Signaling." *Journal of Experimental Botany* 69: 733–740.

Patterson, S. E., J. L. Bolivar-Medina, T. G. Falbel, et al. 2016. "Are We on the Right Track: Can Our Understanding of Abscission in Model Systems Promote or Derail Making Improvements in Less Studied Crops?" *Frontiers in Plant Science* 6: 1268.

R Core Team. 2023. R a Language and Environment for Statistical Computing.

Ramšak, Ž., Š. Baebler, A. Rotter, et al. 2014. "GoMapMan: Integration, Consolidation and Visualization of Plant Gene Annotations Within the MapMan Ontology." *Nucleic Acids Research* 42: D1167–D1175.

Roberts, J. A., K. A. Elliott, and Z. H. Gonzalez-Carranza. 2002. "Abscission, Dehiscence, and Other Cell Separation Processes." *Annual Review of Plant Biology* 53: 131–158.

Schindelin, J., I. Arganda-Carreras, E. Frise, et al. 2012. "Fiji: An Open-Source Platform for Biological-Image Analysis." *Nature Methods* 9: 676–682.

Shannon, P., A. Markiel, O. Ozier, et al. 2003. "Cytoscape: A Software Environment for Integrated Models of Biomolecular Interaction Networks." *Genome Research* 13: 2498–2504.

Sharma, A., H. Samtani, K. Sahu, A. K. Sharma, J. P. Khurana, and P. Khurana. 2023. "Functions of Phytochrome-Interacting Factors (PIFs) in the Regulation of Plant Growth and Development: A Comprehensive Review." *International Journal of Biological Macromolecules* 244: 125234.

Stekhoven, D. J., and P. Bühlmann. 2012. "MissForest—Non-Parametric Missing Value Imputation for Mixed-Type Data." *Bioinformatics* 28: 112–118.

Sundaresan, S., S. Philosoph-Hadas, J. Riov, et al. 2016. "De Novo Transcriptome Sequencing and Development of Abscission Zone-Specific Microarray as a New Molecular Tool for Analysis of Tomato Organ Abscission." *Frontiers in Plant Science* 6: 1258.

Sundaresan, S., S. Philosoph-Hadas, J. Riov, S. Salim, and S. Meir. 2020. "Expression Kinetics of Regulatory Genes Involved in the Vesicle Trafficking Processes Operating in Tomato Flower Abscission Zone Cells During Pedicel Abscission." *Life* 10: 273.

Tanz, S. K., J. Kilian, C. Johnsson, et al. 2012. "The SCO2 Protein Disulphide Isomerase Is Required for Thylakoid Biogenesis and Interacts With LCHB1 Chlorophyll a/b Binding Proteins Which Affects Chlorophyll Biosynthesis in Arabidopsis Seedlings." *Plant Journal* 69: 743–754.

Usadel, B., F. Poree, A. Nagel, M. Lohse, A. Czedik-Eysenberg, and M. Stitt. 2009. "A Guide to Using MapMan to Visualize and Compare Omics Data in Plants: A Case Study in the Crop Species, Maize." *Plant, Cell & Environment* 32: 1211–1229.

Valdovinos, J. G., T. E. Jensen, and L. M. Sicko. 1972. "Fine Structure of Abscission Zones: IV. Effect of Ethylene on the Ultrastructure of Abscission Cells of Tobacco Flower Pedicels." *Planta* 102: 324–333.

Wang, Q., R. W. Sullivan, A. Kight, et al. 2004. "Deletion of the Chloroplast-Localized Thylakoid formation1 Gene Product in Arabidopsis Leads to Deficient Thylakoid Formation and Variegated Leaves." *Plant Physiology* 136: 3594–3604.

Wang, S., and E. Blumwald. 2014. "Stress-Induced Chloroplast Degradation in Arabidopsis Is Regulated via a Process Independent of Autophagy and Senescence-Associated Vacuoles." *Plant Cell* 26: 4875–4888.

Wang, X., K. P. Chung, W. Lin, and L. Jiang. 2018. "Protein Secretion in Plants: Conventional and Unconventional Pathways and New Techniques." *Journal of Experimental Botany* 69: 21–37.

Westphal, S., J. Soll, and U. C. Vothknecht. 2001. "A Vesicle Transport System Inside Chloroplasts." *FEBS Letters* 506: 257–261.

Wilkinson, M. D., M. Dumontier, I. J. Aalbersberg, et al. 2016. "The FAIR Guiding Principles for Scientific Data Management and Stewardship." *Scientific Data* 3: 1–9.

Xu, Y., and Z. Zhu. 2021. "PIF4 and PIF4-Interacting Proteins: At the Nexus of Plant Light, Temperature and Hormone Signal Integrations." *International Journal of Molecular Sciences* 22: 10304.

Supporting Information

Additional supporting information can be found online in the Supporting Information section.